ROTORDYNAMIC AND DRY RUNNING BEHAVIOR OF A FULL SCALE TEST BOILER FEED PUMP

by

Arno Frei

Group Leader Mechanical Development, Pump Division

Johann Guelich

Head of Hydraulic Development, Pump Division

Guenther Eichhorn

Group Leader Product Development, Pump Division

Josef Eberl

Laboratory for Vibration and Acoustics

Sulzer Brothers, Limited

Winterthur, Switzerland

and

Thomas H. McCloskey

Electric Power Research Institute

Palo Alto, California

Arno Frei graduated in 1959 from St. Gall Technical College, Switzerland, with a degree in Mechanical Engineering. He joined Sulzer in 1966, and was first engaged in the design and development of primary recirculation pumps for nuclear power station. After activities in the field of nuclear heat exchangers, he rejoined the pump division, where he has been head of the mechanical development group since 1978.

Mr. Frei has a degree in Mechanical Engineering from St. Gall Technical College (1959). He has taken continuing courses in Mathematics/Mechanics from Winterthur Technical College (1962-1965) and Federal Institute of Technology (ETH) (1967-1971). He attended courses in Fluid Mechanics, Thermodynamics, Turbomachinery at (ETH) (1972-1974) and is continuing his studies in Applied Mathematics/Mechanics at ETH.

Johann Guelich obtained an M.S. degree in Mechanical Engineering at the Technical University of Hannover, Germany, and a Ph.D. at the Technical University of Darmstadt, Germany. In 1965-1966, he worked on nuclear power station projects for Siemens. From 1967 to 1978, he headed a group responsible for the thermohydraulic design of nuclear boilers and heat exchangers. Since 1979, he has been head of the Hydraulic Development Group of the Sulzer Pump Division.

Guenther Eichhorn graduated in 1953, from Ilmenau Technical College, Germany, with a degree in Mechanical Engineering. In 1959, he joined Sulzer and was engaged in the design of various types of centrifugal pumps. Since 1968, he has been one of the leaders in the design department and is responsible for Product Development of Pumps for Power Generation.

ABSTRACT

Excessive rotor vibrations are one of the leading causes of damage to pump components, particularly to bearings, shaft seals, and premature wear of labyrinth surfaces.

Under an EPRI contract which was awarded to Sulzer in 1983, a full scale three-stage test pump was built which has been extensively tested for rotordynamic behavior. Design conditions selected for this pump are typical for fossil plants with subcritical steam generation. The pump was installed in a closed loop.

To investigate rotordynamic behavior experimentally, the pump had to be equipped with sophisticated instrumentation including shaft vibration measurements within the pump.

The influence of different parameters such as labyrinth clearances, amount of unbalance, swirl brakes, and flowrate is described. Experimental results (i.e., unbalance response) are compared with analytical results using a rotordynamic code based on finite element approach.

In boiler feed pump systems, for a number of reasons, sudden loss of suction pressure can occur. In such cases, vaporization in the pump occurs accompanied by two phase flow conditions, large hydraulic forces, loss of damping, high rotor amplitudes, with possible contact between rotor and stator. This condition was simulated with the test loop. The influence of such a loss of

suction incident on pump behavior, especially shaft vibrations, is described.

The conclusions highlight the importance of the labyrinths on rotordynamic behavior, in particular the influence of swirl brakes to reduce shaft vibration amplitudes.

If the analytical results have to compare well with measured vibrations, excellent quantitative knowledge of bearing, labyrinth and impeller interaction dynamic coefficients is essential.

INTRODUCTION

Rotordynamic behavior is one of the most important criteria for the reliability of boiler feed pumps. Among turbopumps, boiler feed pumps are unique for their high power concentrations [1]. During the design stage of such pumps, the influence of all rotor elements like bearings, impellers, impeller labyrinths, balance piston, shaft seal, and couplings on rotordynamic behavior has to be evaluated very carefully. Otherwise, vibration phenomena may arise during pump operation which drastically reduce pump availability. Quite often, such phenomena are related to self excited rotor vibrations [2, 3]. During the last decade, great efforts have been made by pump industry and university laboratories in achieving a better understanding, both qualitatively and quantitatively, of the rotor vibration phenomena occurring in a pump. An overview is given by Bolleter, et al. [4]. Investigators have worked both theoretically and experimentally on the different rotor elements, e.g. [5, 6, 7, 8, 9, 10].

Rotordynamic computer programs have evolved also. The earlier computer codes based on the transfer matrix method have been superseded by more efficient codes with better numeric stability, based on the finite element approach. Such programs allow for damped eigenvalue and forced vibration analysis, some of them for both lateral and torsional vibrations [11, 12, 13]. Therefore, good tools are available today for predicting the rotordynamic behavior of multistage pumps. However, such calculation models should be compared with the real behavior of a pump in a test. To provide such benchmark tests was one of the objectives when building a ten megawatt boiler feed pump under an EPRI sponsored research contract.

Testing the rotordynamic behavior of a pump is difficult for two reasons:

- Pump rotors of multistage pumps typically exhibit a high amount of damping. Therefore, amplification is small, hence, resonance peaks are flat. It is, thus, very difficult to detect any natural mode with its associated frequency and modal damping values by either unbalance excitation or by impact excitation, i.e., experimental modal analysis. The phase shift during a runup or rundown test is typically the only indication of a resonance situation.

One way to detect a natural mode of the rotor is by running it at or even slightly beyond the stability limit. This can be due to clearance enlargement in service [2, 3], or with artificially enlarged clearances on the test bed [14].

A frequency analysis of the shaft vibration will then exhibit the frequency of the least damped, unstable mode, and the damping is known to be about zero at the stability limit. This method is not generally applicable, however.

- Because of easy accessibility rotor vibrations are measured typically by proximity probes near the journal bearings. Measuring shaft vibration within the active part of a pump (impellers, balance piston) is an elaborate task, because the proximity probes to be installed must be watertight and have to withstand temperature and pressure inside the pump. However, for a conclusive comparison between test and analysis such internal shaft vibration measurements are absolutely essential.

For the test pump, it was decided to run the tests.

- in the "as built" condition.
- with known test unbalances at the driving coupling and at the balance piston.
- with "design" internal clearances.
- with artificially enlarged (twice "design") clearances.

To determine the response due to the effect of the test unbalances only, the vector differences between the two runs "with test unbalances" and "as built" have to be established. This implies that the residual unbalance condition remains the same for the two runs. Therefore, fitting the test unbalances shall not require dismantling of the rotor.

Another important task which had to be investigated with the test pump was its behavior during severe transient conditions. In boiler feed pump systems, due to a number of reasons, sudden loss of suction pressure can occur. In such cases, vaporization in the pump takes place accompanied by two phase flow conditions, large hydraulic forces, loss of damping, and possibly high rotor amplitudes, contact between rotor and stator and potentially severe damage to the pump. Some specifications require, therefore, that the boiler feed pumps should survive such short time "vapor locked" or "dry running" conditions without too much harm and with minimum wear.

The influence of "loss of suction pressure" on shaft vibration behavior can, as a transient condition with severe random excitations between full flow and vapor lock, hardly be modelled in an analytical way. It is, therefore, the test which gives the answer how far such a condition can be sustained by the rotor. In addition, the character and magnitude of the excitation can be deduced from the rotor response. The tests carried out had the aim of answering the following questions:

- What shaft amplitudes develop during the transient?
- How does the frequency spectrum look like?
- Will the shaft vibrations cause damage to bearings and internal clearances?
- What shaft amplitudes show up when the shaft is run through the "dry critical speed" in the vapor locked condition?

TEST EQUIPMENT

Test Pump

Design data selected for the test pump is given in Table 1. These data are typical for fossil fired power plants with subcritical steam condition.

It was decided to build a three-stage pump, with a head per stage of 800 meters (2623 ft). This results in a compact pump design, and a head per stage which exceeds most of today's applications.

A longitudinal section through the pump is shown in Figure 1. In the following, the main features of this pump are described:

- *Pump Casing/Baseplate*—The casing is a forged barrel with suction, discharge and intermediate take off branches welded on. The casing is supported by heavy welded on lugs on centerline level. A rigid, welded baseplate design has been chosen. Guide trunnions at the bottom of the pump casing ensure axial and transverse fixation to the baseplate and at the same time allow for free thermal expansion of the casing. The plate is designed to take up forces and moments acting on the casing and assure safe transmission to foundation, conceived to avoid casing baseplate resonances within the operating speed range of the pump.

- *Discharge Cover*—Forged flangetype cover with a heavy stud connection designed for hydraulic tightening (tensioners). The seal is accomplished by a spiral wound gasket.

Table 1. Main Data of Pump.

Hydraulic Data		
Q	(m^3/s)	0.37
at BEP	(gpm)	5865
n	(rpm)	8080 max.
H_{tot}	(m)	2400
	(ft)	7870
H_{stage}	(m)	800
	(ft)	2623
T	(°C)	180 max.
	(°F)	356
eta	(−)	0.83
Geometrical Data		
Bearing Span		1406 mm (55.4 in)
Impeller Diameter		307 mm (12.1 in)
Shaft Diameter		124 mm (4.9 in)
Rotor Mass		300 kg (662 lb)

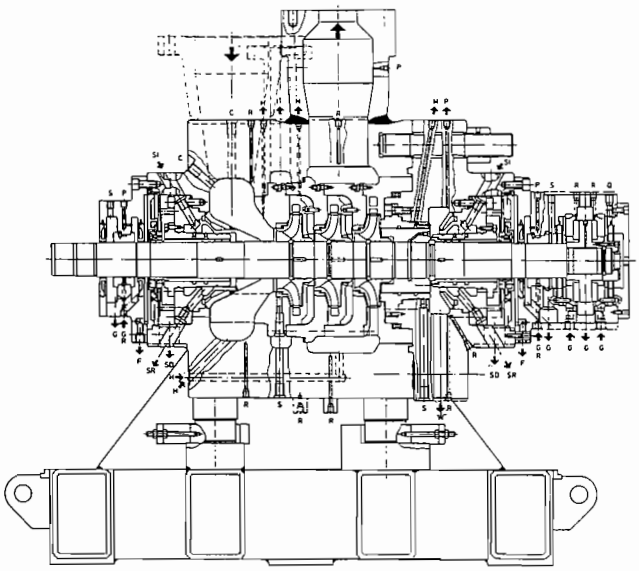

Figure 1. Pump Longitudinal Section.

• *Internal Element*—The internal element consists of rotor, diffusers, and radially split stage casings, and can be mounted as a unit into the pump casing. It is axially pushed against the two casing shoulders by the discharge cover, through a seal pack consisting of a number of spiral wound gaskets, plus spacer rings which compensate relative thermal expansions.

• *Thrust Balancing Device*—The main hydraulic thrust is balanced by a straight balance piston. The bore of the liner has helical grooves to reduce leakage, along with two deep circumferential grooves to optimize radial stiffness behavior and to reduce the detrimental effect of rotor tilting on radial stiffness. A swirl brake has been located at the entrance to the throttling clearance. This swirl brake consists of numerous radial bores in the liner near the entrance, feeding the water into a circumferential groove with almost zero prerotation [17]. The residual thrust is carried by a double acting tilting pad thrust bearing with directed pressure oil lubrication.

• *Journal Bearings*—These are fixed four-lobe bearings, pressure oil lubricated. They are mounted in bearing housings with 360 degree fixation to casing and cover. Bearing housings and bearings are axially split.

• *Rotor*—Impeller fixation on shaft by shrink fits allows free axial thermal shaft expansion, assures interstage sealing and good concentricity, and allows maximum possible shaft diameter. Double keys are provided to take up torque during thermal transient conditions. Split rings assure a correct axial position and take up axial thrust during transient conditions. Balance piston, thrust bearing collar and coupling hub are fixed to the shaft by means of shrink fits without keys. Balance piston and thrust collar are positively locked in axial direction with split rings. There are no threads on the shaft.

• *Shaft Seals*—Fixed throttling bushes with injection and relief to deaerator or preheater are used. Shaft sleeves in way of throttling clearance are provided with helical grooves to reduce leakage. The throttling bushes are located in cooling housings.

Test Setup

The test stand arrangement is shown in Figure 2.

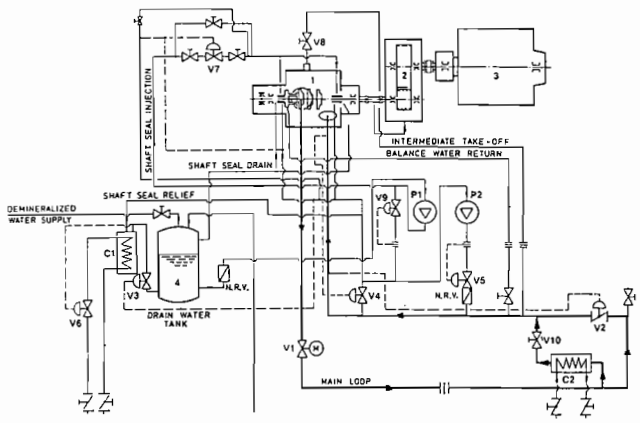

Figure 2. Test Loop Layout.

• *Pump Driving Train*—The pump is driven by an electric motor with a rated output of 8400 kW, operating in the speed range between 900 and 1500 rpm. A speed increasing spur gear with a gear ratio of 5.43 allows for a pump speed range between 4900 and 8100 rpm. A membrane coupling with reversed hub (low moment type) was selected to transmit the torque from gear pinion to pump shaft.

• *Main Loop*—The water is pumped in a closed loop from the main pump discharge through the motor driven main throttling valve V1, a flow measurement orifice, the motor driven suction temperature control valve V2, and back into the main pump suction. The water temperature in the main loop is controlled by cooler C2, connected in parallel to valve V2. The pump is de-

signed with an intermediate take off connection after the first stage. The water is flowing from the pump through a throttling valve and a flow measuring orifice back into the main loop downstream of valve V2. The leakage along the balance piston is collected in the balancing chamber and flows back through a flow measuring orifice into the suction part of the main loop.

• *Pressure Control System*—Three pressure levels must be maintained by the complex pressure control system:

· 30 bar in the suction part of the main loop

· 12 bar in an intermediate circuit simulating the deaerator

· atmospheric pressure in a water tank collecting shaft seal leakage

Two auxiliary pumps, P1 and P2, together with the necessary control valves, maintain the above pressures.

· Shaft Seal injection and relief water is taken after pump P1 at a pressure slightly higher than 12 bar, and injected via a control valve into the two shaft seals. Water is drained into the 12 bar line from an intermediate chamber along the throttling bush of each seal, situated between the seal injection chamber and the balancing, respectively suction chamber. By this system, injection of cold water into the pump can be avoided during operation.

Rotordynamic Instrumentation

Besides flow quantities which were measured at various places in the loop system, pressures and temperatures have been measured at numerous locations in the pump. Radial rotor displacements were measured at five different locations (Figure 3):

- At the coupling
- Outboard of the drive end journal bearing
- At the suction impeller labyrinth
- On the balance piston near the balance chamber
- Outboard of the non-drive end journal bearing

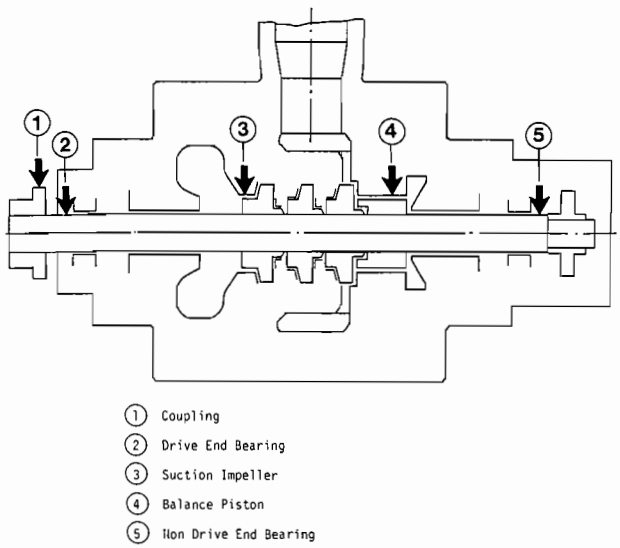

Figure 3. Proximity Probe Locations along the Rotor.

At each of the above five measuring planes, pairs of proximity probes were installed 90 degrees apart. Whereas, the probes installed at coupling and journal bearings were commercially available eddy current probes, the probes installed inside the active pump part had to be developed to be watertight at a temperature of 180°C and a pressure of 35 bar. After some initial failures, this aim was successfully achieved. An eddy current probe installed at the coupling provided the once-per-revolution pulse necessary as phase reference for the extraction of vibration vectors. Accelerometers measuring bearing housing vibrations were also installed.

An essential part of the data handling is a 16 channel pulse code modulation (PCM) recording system. After appropriate transformation and amplification to fit the input requirements, all transducer signals are fed to the PCM modulator with 12 bit amplitude resolution. The output of this modulator is a single digital signal which is recorded on a standard VHS video cassette. The digital processing limits the frequency band width of the data records to a usable range of 2500 Hz. The analysis of the test data is organized as an offline task. Digital signals from the video tape are reproduced in a 16-channel PCM demodulator which comprises an error correction circuit to compensate for tape imperfections. A computer controlled analysis and data storage instrumentation is connected to the output of the demodulator.

ROTORDYNAMIC TESTS

Test Procedures and Data Processing

For each test point (as defined by the test configuration, flowrate referred to best efficiency point and temperature) the orbit was measured during a speed ramp of three to four minutes duration. For each flowrate the ramp was run from about 7900 rpm down to 4800 rpm and back again.

The evaluation of the test data was basically done in two ways:

• Extraction of the synchronous vibration vectors at certain speed intervals. A two channel vector filter was installed for this task.

• Frequency analyses at certain speed intervals to yield frequency cascade diagrams. A two-channel FFT analyzer was used for the extraction of this frequency domain information.

The setup of both instruments and the data readout were controlled by a desktop computer, which in turn stored the rpm-correlated vectors and frequency spectra on a disk drive for later presentation in various forms of vector diagrams and frequency cascades, respectively.

Test Program

The following parameter variations were investigated during the rotordynamic tests:

- Flowrate as a fraction of best efficiency flow
- Increased unbalance
- Operation at 80°C and 160°C
- Increased clearances at labyrinths and balance piston
- Swirl brake at balance piston
- Increased clearance at throttling bush shaft seals

In order to compare measured vibration amplitudes with the values calculated by a computer code for forced response, the test has to be run with a known unbalance.

The following additional unbalances have been installed:

at coupling	1450 gmm	(2.01 ounce-in)
at balance piston	3820 gmm	(5.30 ounce-in)

These unbalances are quite high and correspond to an ISO balance quality G = 16.

The additional unbalances were mounted 180 degree out of phase, in order to excite the first bending mode. Since the unbalance of the original rotor and the hydraulic excitation forces

were not known with respect to size, distribution, and phase, the additional unbalance did not necessarily increase maximum amplitude, but changed, of course, the vibration vector. Only these differential vectors, between the runs with and without the additional unbalances, provide a meaningful comparison of the test results with the calculation.

Test Results

Each pair of vibration probes provided two signals from which the orbital movement of the shaft was determined. To derive the frequency spectra, the unfiltered signals were used. If all non-synchronous frequencies are filtered out, the orbit shows up as an ellipse (Figure 4). The lag between the high point of one of the signals and the trigger mark on the shaft gives the phase angle.

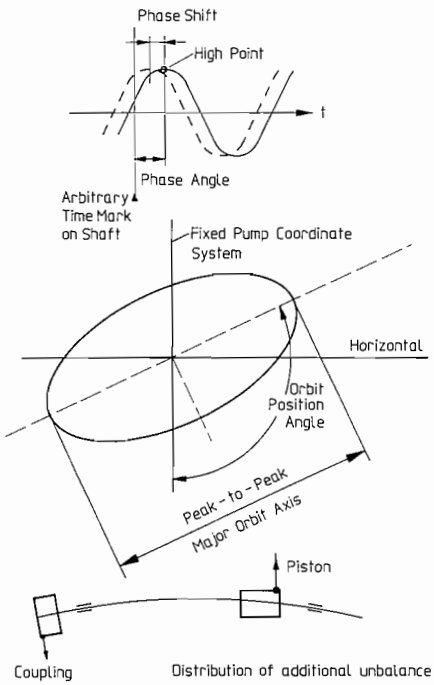

Figure 4. Definition of Vibration Parameters.

The filtered vibration diagrams are presented in the following form:

- Mechanical and electrical runout is compensated.
- Diagrams show the peak-to-peak amplitude of the major orbit axis and the phase angle (Figure 4).

Shaft vibrations in the five measuring planes are shown in Figure 5 for the pump "as built," at 160°C, and BEP flow. Peak-to-peak amplitudes at the bearings are up to ten μm and attain 30 μm at impeller, balance piston and coupling. Amplitudes are thus very low. There is little phase shift across the shaft speed range.

The shaft vibrations shown in Figure 6 have developed at twice the design labyrinth clearances. At the bearings, the amplitudes still do not exceed ten μm, but they attain 100 μm at the impeller, 65 μm at the balance piston, and 35 μm at the coupling. Phase shift becomes more pronounced—50 degrees at the impeller and 90 degrees at the drive end bearing.

The shaft orbit is shown in Figure 7 at the impeller for the same operating conditions as for Figure 6. The orbit is nearly circular. The amplitude/phase loci indicate a resonance situation at

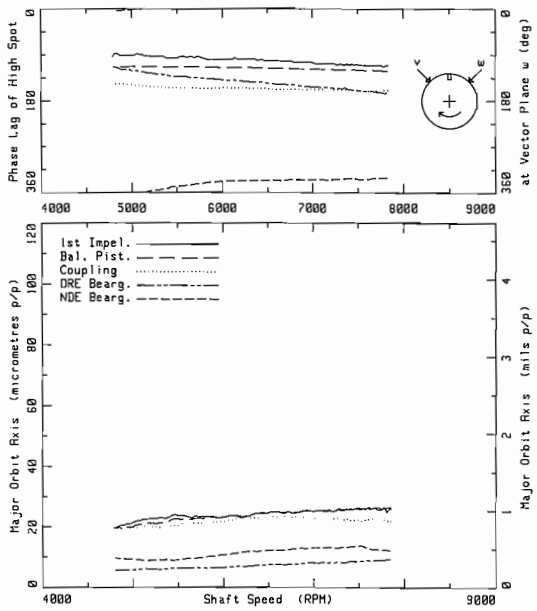

Figure 5. Shaft Vibrations with Nominal Clearances (Pump as Built).

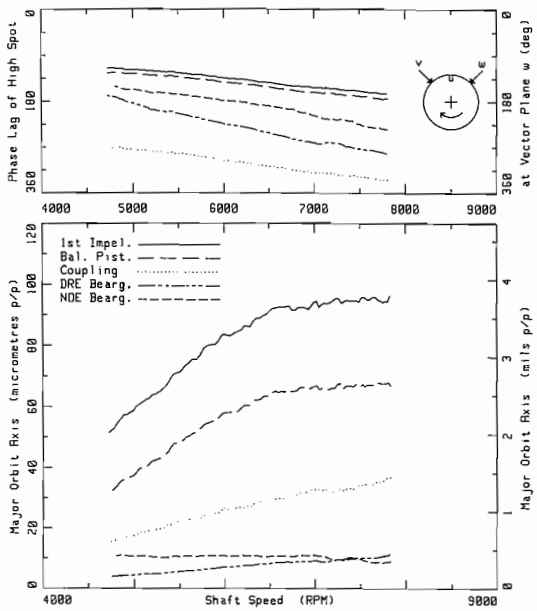

Figure 6. Shaft Vibrations with Two × Nominal Clearance at Impellers and Balance Piston.

the upper end of the speed range, which, however, is heavily damped.

In the following diagrams, the influence of different parameter variations on the impeller vibration amplitude is shown. The influence of the flowrate is shown in Figure 8. It can be seen that this influence is small, except at 25 percent BEP flowrate, where the amplitude drops by about 20 μm at 6500 rpm. This can be explained by changing flow conditions at the rear shroud of the last impeller, due to recirculation between impeller and diffuser, which has a similar effect as a swirl brake in front of the balance piston [16].

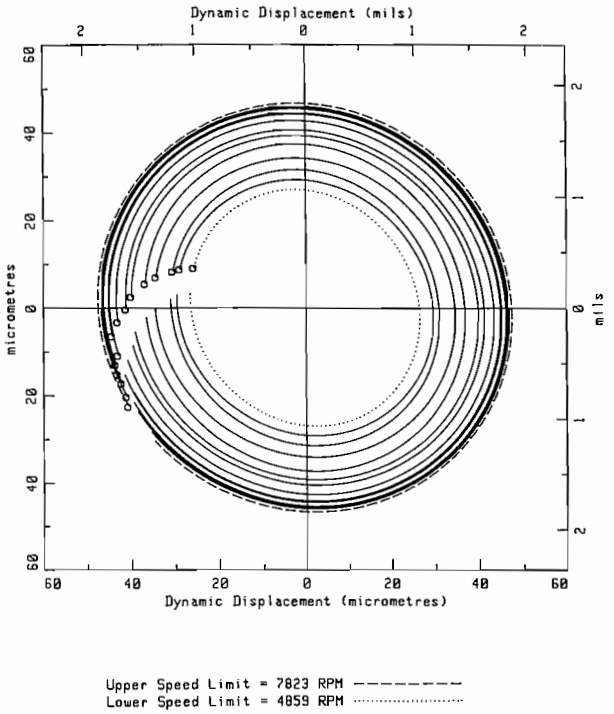

Figure 7. Filtered Shaft Orbit with Two × Nominal Clearance at Impellers and Balance Piston.

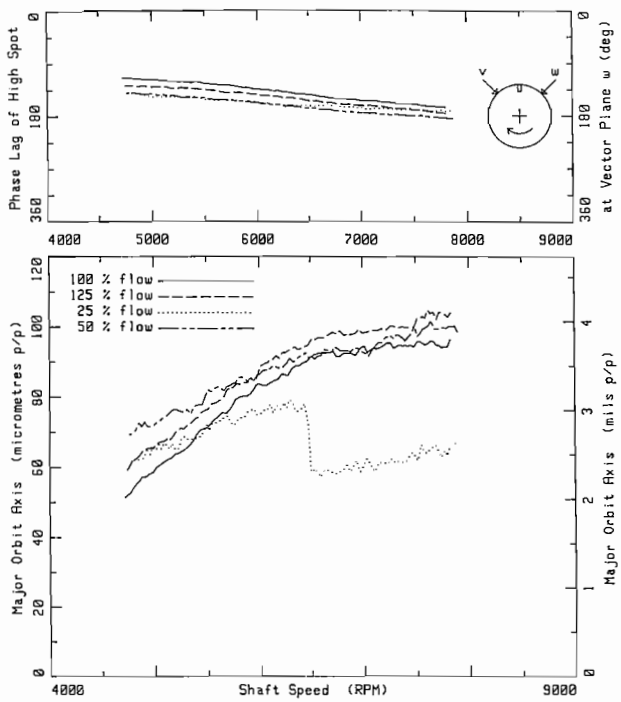

Figure 8. Shaft Vibration for Different Flowrates with Pump Having Two × Nominal Clearance at Impellers and Balance Piston.

The effect of additional unbalances as stated in the test program is reflected in Figure 9. Interestingly, the maximum amplitude decreases, but the phase curves clearly show a turning of the vibration vector, which indicates that the additional unbalances are not in phase with the residual mechanical and hydraulic unbalances. Evaluation of these measurements shows that unbalance excitation in the rotor "as built" is of the same magnitude as from the additional unbalances which are quite large.

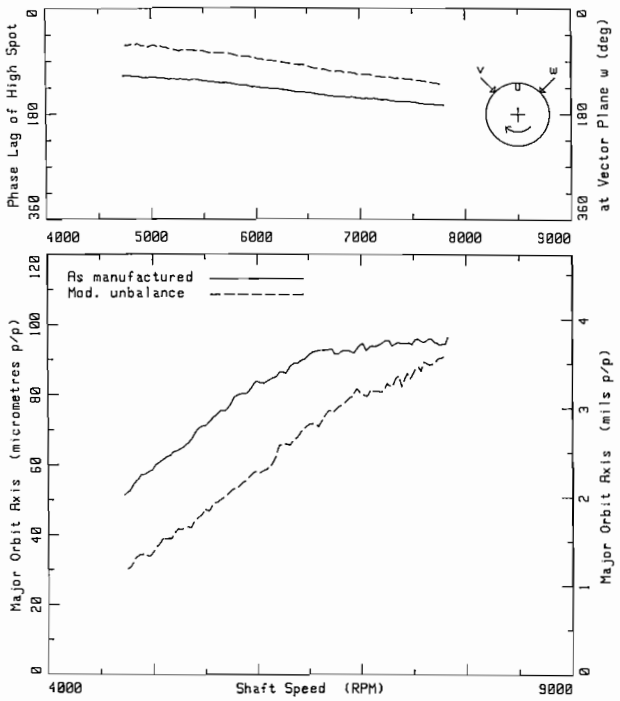

Figure 9. Unbalance Response of Shaft Vibrations with Pump Having Two × Nominal Clearance at Impellers and Balance Piston.

As the rotor was balanced mechanically very well, this can only be explained by considerable hydraulic unbalance forces (hydraulic excitation forces running synchronously with the shaft) being present even with the high quality precision cast impellers installed. The magnitude of the hydraulic unbalance force corresponds quite well to other measurements carried out [10]. With the definitions and numbers given in this reference, the hydraulic unbalance per impeller is estimated to be 1200 to 1800 gmm (1.66-2.5 oz-in).

Thus, the three impellers together will develop hydraulic unbalance forces of the same magnitude as the additional unbalances installed. In contrary, the residual mechanical unbalance of the assembled rotor was 500 gmm (0.69 oz-in), which corresponds to a balance quality between G1 and G2.5, according to ISO Standard 1940.

The strong effect is shown in Figure 10 of a swirl brake at the balance piston entrance (a device which removes the circumferential water velocity component) on vibration amplitudes. These are cut down to about 50 percent of their original values. This is due to the increased resultant rotor damping which originates from the reduced driving forces as a result of the swirl brake action.

The influence of water temperature on the synchronous vibration component was rather insignificant.

At enlarged clearances, pump rotors typically are prone to subsynchronous, self excited vibration. It was, thus, of utmost interest whether this pump would show, at twice design clearances and without a swirl brake installed, any sign of such an instability.

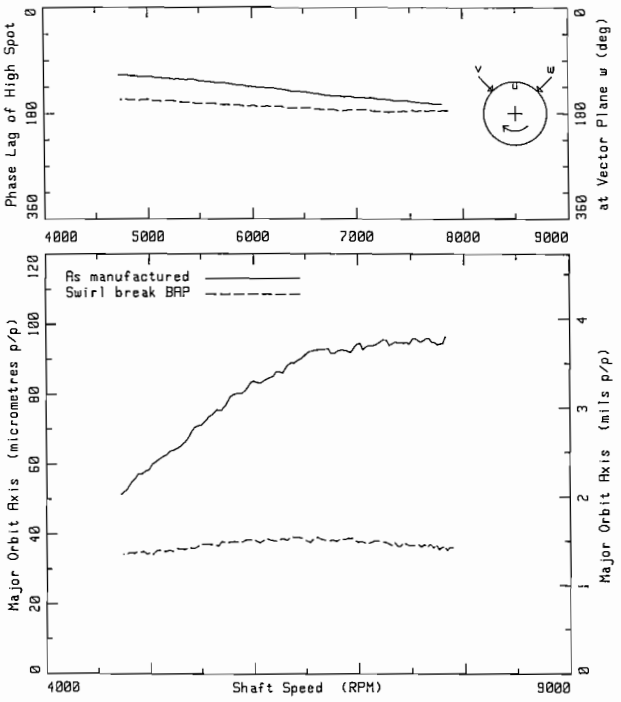

Figure 10. Reduction of Shaft Vibrations Due to Swirl Break at Balance Piston.

Frequency spectra of unstable pump rotors are shown in previous studies [3, 14].

The frequency cascade for the test pump under the above mentioned conditions is shown in Figure 11, for 25 and 100 percent of BEP flow. There is no sign of an instability whatsoever, indicating a very stable rotor design.

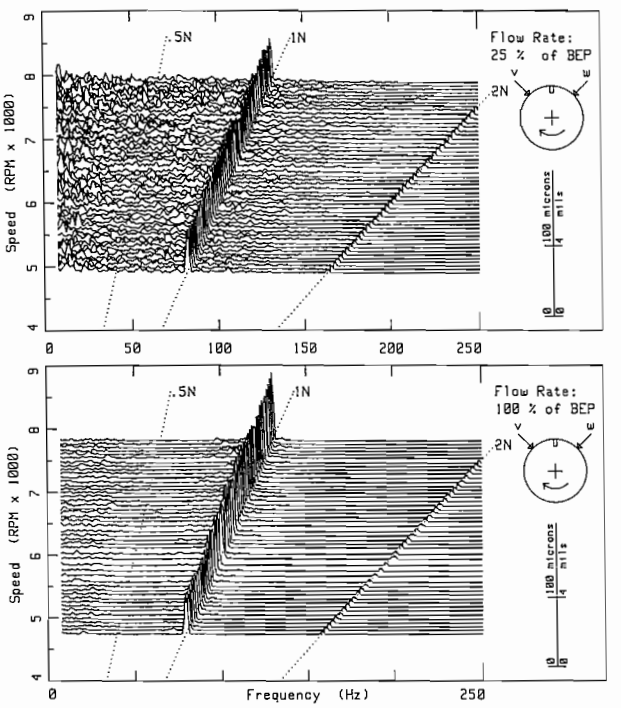

Figure 11. Uncompensated Shaft Vibrations (Vector V) with Two × Nominal Clearance at Impellers and Balance Piston.

Synchronous response from unbalance excitation dominates. Subsynchronous response from broad band excitation due to turbulence and backflow is present at part load, as being expected.

Discussion of Test Results

In a strict sense, the conclusions that can be drawn from the test results are valid only for the test pump, which is of a short, rigid design. Nevertheless, they are basically true also for pumps with a higher number of stages. However, in order to ensure good rotordynamic behavior, similar calculations as outlined should be performed.

- For the pump in the "as designed" condition, shaft vibration amplitudes are very low.
- For twice design labyrinth clearances, vibration amplitudes increase considerably, but still remain far below the clearance value. Synchronous response is dominating. In fact, no subsynchronous vibrations indicative of instabilities could be observed during the test.
- Comparison of the tests with and without additional unbalance indicates that a high percentage of the synchronous response originates from hydraulic unbalance, i.e., hydraulic forces which are proportional to stage head and rotate with the impeller. This is due to tolerances of the impeller channels (even though precision cast impellers were used).
- The positive influence of swirl brakes on rotor vibrational behavior is again confirmed. It is demonstrated that unbalance response can be drastically reduced by introducing a swirl brake at the balance piston entrance. Although the influence of this swirl brake on self excited vibration could not be demonstrated, it is well known [2, 3] that such a device can bring an unstable rotor back to stability.

ROTORDYNAMIC ANALYSIS

Model

The rotor was modelled using the MADYN computer program [11] together with an inhouse developed pre/postprocessor. The MADYN program is a finite element based program which will accept nonsymmetric stiffness and damping matrices, gyroscopic forces, harmonic and transient excitation. Reactive forces on the rotor are described in the well known linear manner as stiffness, damping, and mass matrices [14]:

$$-\begin{bmatrix} F_1 \\ F_2 \end{bmatrix} = \begin{bmatrix} K_{11}\ k_{12} \\ k_{21}\ K_{22} \end{bmatrix} \begin{bmatrix} X_1 \\ X_2 \end{bmatrix} + \begin{bmatrix} C_{11}\ c_{12} \\ c_{21}\ C_{22} \end{bmatrix} \begin{bmatrix} \dot{X}_1 \\ \dot{X}_2 \end{bmatrix} + \begin{bmatrix} M_{11}\ m_{12} \\ m_{21}\ M_{22} \end{bmatrix} \begin{bmatrix} \ddot{X}_1 \\ \ddot{X}_2 \end{bmatrix} \quad (1)$$

Dynamic stiffness of the bearing supports was considered large compared to the oil film.

Input Data

Selected geometrical data for journal bearings, seals and impellers are given in Table 2.

The coefficients for the labyrinths and balance piston were calculated with a computer program based on Nordmann's theory [6]. The tangential velocity of the leakage flow along the impeller shroud was calculated by an integration with finite differences, taking different roughnesses of the rotating and stationary parts into account. The pressure was reduced according to water rotation to yield the pressure difference across the seal.

Stiffness and damping coefficients for the journal bearings are based on dimensionless data provided by the bearing manufacturer. The data for impeller interaction forces was derived from testing described in [10].

Table 2. Journal Bearing and Seal Data.

Location	Diameter (mm) (in)	Length (mm) (in)	Diametral Clearance (mm) (mils)	Remarks
Bearing	115 4.5	60 2.4	0.15 5.8	
First stage suction	230/215 9.1/8.5	12/18 0.47/0.71	0.55 21.6	Stepped
Normal stage suction	220/205 8.7/8.1	12/18 0.47/0.71	0.55 21.6	Stepped
Inter-stage seal	150 5.9	16 0.63	0.55 21.6	Straight
Piston	218 8.6	166 6.5	0.44 17.3	Divided by grooves
Shaft seal	145 5.7	220 total 8.7	0.42 16.5	3 Sections

Results of Calculation

An overview of the three cases analyzed is given in Table 3. Damped natural frequencies as well as unbalance response have been calculated.

Table 3. Cases for Rotordynamic Analysis.

Case	Seals	Swirl brake[2]	Flow	Additional unbalance	Water temperature
1	new	no	BEP	yes	160°C
2	worn[1]	no	BEP	yes	160°C
3	worn[1]	yes	BEP	yes	160°C

[1] Twice "new"
[2] At balance piston entrance

Damped natural frequencies are most interesting for case two and are shown as a Campbell plot in Figure 12. Critical speeds occur where an eigenfrequency coincides with the running frequency, represented by the straight line. It is shown that natural modes near running frequency are well damped. Damping is defined as

$$D = \text{Critical damping ratio} = \frac{-\text{Re}(\lambda)}{[(\text{Re}(\lambda))^2+(\text{Im}(\lambda))^2]^{0.5}} \qquad (2)$$

where λ is the complex eigenvalue [14].

The least damped mode shows sufficient stability margin throughout, which agrees with the fact that no self excited vibration was observed in the test for this case. The good damping properties even at twice design clearance are to a certain extent the merit of the fixed throttling bushes which add damping to the system.

Calculated unbalance response at the impeller location as a function of shaft speed is shown in Figure 13 for the three cases. There is no sign of a resonance peak in the speed range covered by the analysis.

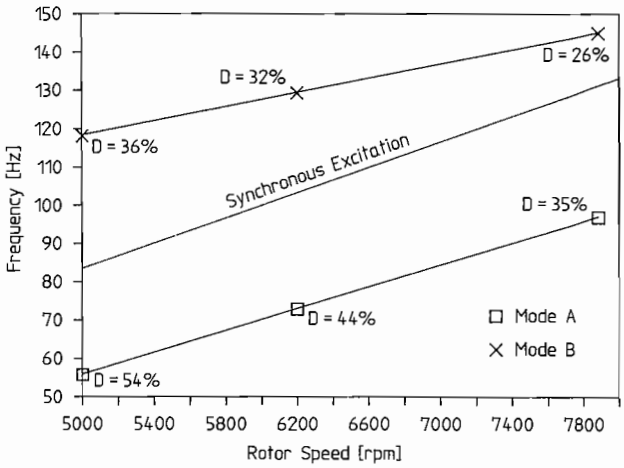

Figure 12. Campbell Diagram for Case 2.

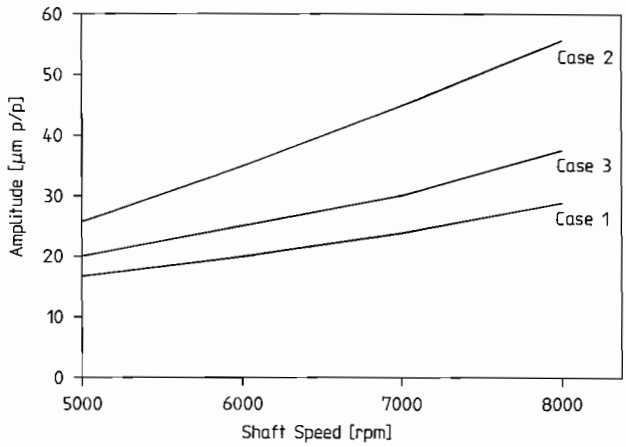

Figure 13. Calculated Unbalance Response at the Impeller.

COMPARISON TEST/ANALYSIS

As mentioned in the introduction, only vector differences between the vibration vectors of the test runs with and without additional unbalances can be compared with the calculated unbalance response.

For case two, this comparison is shown in Figures 14 through 17, for drive end bearing, impeller, balance piston and non drive

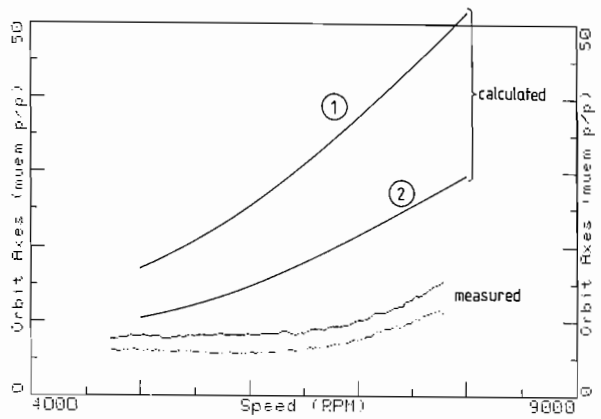

Figure 14. Comparison Test/Analysis, Case 2: Drive End Bearing.

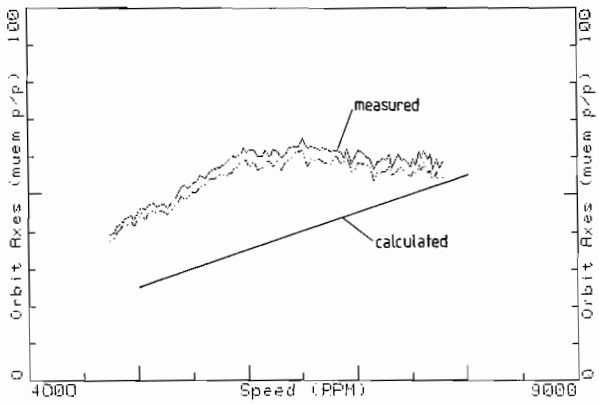

Figure 15. Comparison Test/Analysis, Case 2: Impeller.

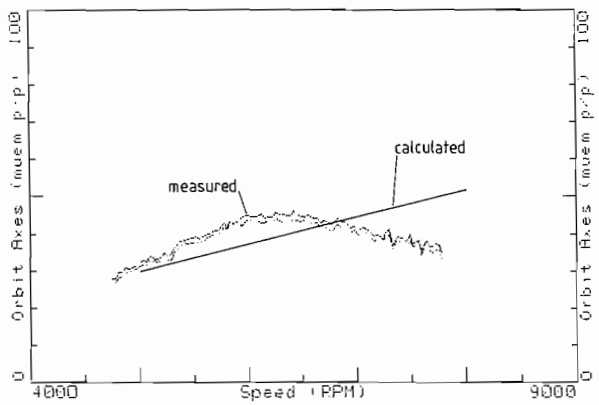

Figure 16. Comparison Test/Analysis, Case 2: Balance Piston.

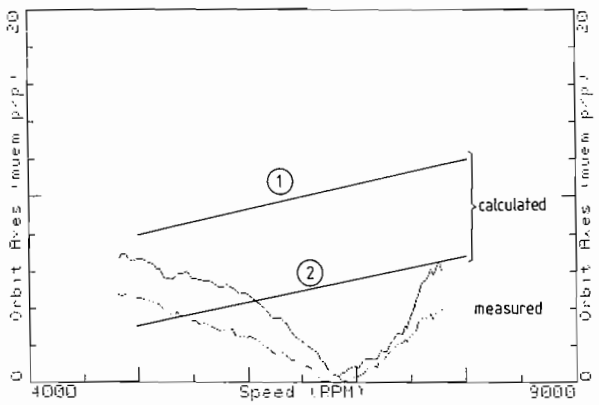

Figure 17. Comparison Test/Analysis, Case 2: Non Drive End Bearing.

end bearing locations. For impeller and balance piston the agreement is reasonable.

Remaining discrepancies are thought to be due mainly to uncertainties of the rotordynamic coefficients of the seals and the balance piston. Ongoing experimental and theoretical work under the EPRI contract is expected to yield improved data. At the bearings, the assumed static loading strongly influences the calculated response. This load typically is not well known. If the bearings are assumed to be loaded just by rotor weight, the agreement between test and analysis is poor, but becomes better if higher loadings are assumed. The reason for this behavior is the strong dependence of the bearing coefficients (stiffness, damping) on static load. Higher loadings can in fact be expected when the bearing centers are set higher than the internal labyrinth centers, which is common practice for boiler feed pump assembly. In contrast, the annular seal coefficients (impeller seals, balance piston, fixed throttling bush) depend only marginally on the static rotor position up to an eccentricity of about 50 percent of the clearance [18].

DRY RUNNING

Modifications to Test Equipment

In principle, the same test pump, test loop, and instrumentation as described above was used for the dry running test. One modification was made to the test pump. Because higher excitation forces and, consequently, larger rotor amplitudes had to be expected, the running clearances were opened up by 30 percent when compared with the design clearances given on Table 2.

A modification was necessary on the test loop also. In order to simulate the dry running condition, a bleedoff line was installed between the balance water return and the test bed reservoir, which enabled to drain the pump.

Test Procedure

Steady operating conditions were established at a speed of 7900 rpm at 25 percent of BEP flow, 160°C water temperature and 30 bar inlet pressure. To initiate the loss of suction transient the inlet pressure was reduced by shutting down the second stage auxiliary pump and by opening the relief valve venting the test loop to the water basin. This valve remained open until the test loop was completely empty and the test pump was running dry.

Test Results

The total static pressure differential Δp developed by the pump, the water temperature in the suction pipe, and the available NPSH, are shown in Figure 18 as a function of time. The sequence of events shown in Figure 18 can be described as follows:

- t = 0 min corresponds to steady conditions prior to the loss of suction transient.
- At t = 1 min, the suction pressure was reduced by shutting down the auxiliary pump used to create the required suction pressure during normal operation. The NPSH available dropped immediately by about 120 m.
- At t = 1.5 min the drain valve was opened in order to create a loss of suction condition. Three percent head drop (NPSH three percent = 60 m) was reached at about t = 2.2 min.
- Head breakdown occurred at about NPSH = 20 m. This condition was reached at about t = 9 min.
- Subsequently, large surge like fluctuations of the discharge pressure were recorded from t = 9 min to about t = 13.5 min. The amplitudes increased during this period to up to 150 bar peak-to-peak.
- At t = 14 min, these fluctuations stopped suddenly and completely and the pump was now running in steam. At t = 14.7 and 20.5 min, a "gulp" of water entered the pump, apparently from somewhere in the loop (may be seal injection water). This caused the sharp peaks of the discharge pressure.

Vibration amplitudes in the five measuring planes discussed earlier were recorded continuously during the entire transient. In order to bring out clearly the most violent peaks of the rotor vibrations, spectra were established in the "peak-hold" mode. Five vibration spectra in Figure 19 are shown established in this

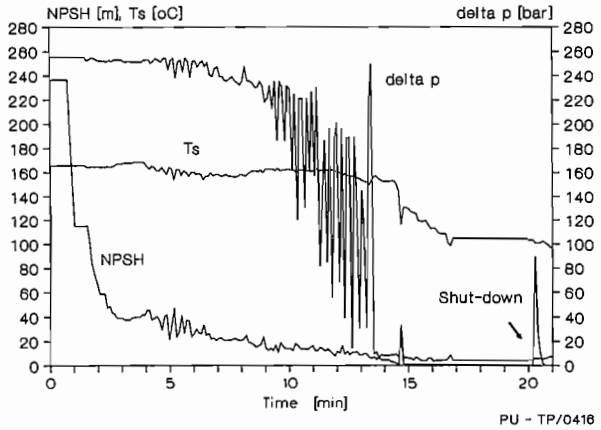

Figure 18. Dry Running Test: Time History.

mode and recorded over two min each at different periods during the transient. These periods correspond to the initial steady operation conditions prior to the transient, to the period with low pulsations (t = 7 to 9 min), to the heavy pulsations t = 12 to 14 min, to the transition period at t = 14 to 16 min, and to operation in steam t = 17 to 19 min. The vibration amplitudes are peak-to-peak values measured at the suction impeller. During all of above periods, the peak at rotational frequency remained between 30 and 40 μm peak-to-peak, indicating that no appreciable hydraulic unbalance was created by the two phase flow in the impellers. During the period of heavy fluctuations, the highest vibration peaks at the impeller reached 42 μm p-p. Only during the transition to empty conditions peaks of 65 μm p-p were recorded. No critical speed was observed even during running in steam, since the rotor is short and stiff and well balanced.

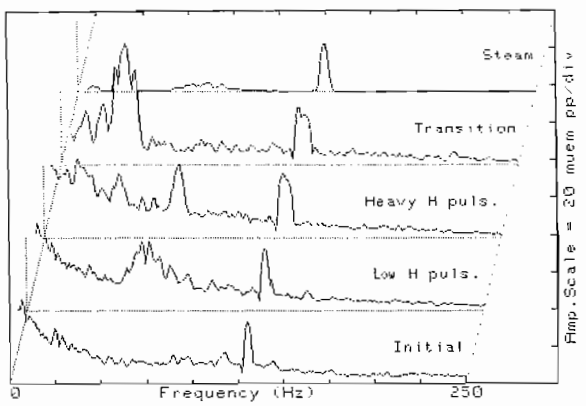

Figure 19. Frequency Spectra of Shaft Vibrations at Impeller.

After several minutes of operation at the dry condition, the pump was switched off accompanied by a measurement of the rundown time and then left for complete cooling down.

One day later, the pump was restarted and run up to full power, in order to compare the running behavior with the previous test. It was confirmed that no measurable change had occurred.

Finally, the pump was dismantled and inspected for possible damages. No wear of the labyrinths and no degradation of any component of the pump could be detected.

Discussion of Test Results

The requirement of dry running is not usually found in boiler feed pump specifications (although some clients have such a request). The very rugged pump reported here, however, was designed for such extreme requirements, such that even the 30 percent enlargement of the clearances was considered unnecessary after analyzing the test results. Obviously, the results obtained are specific for this design, and good engineering judgement is necessary when applying these results to pumps with a larger number of stages or to different designs.

As mentioned earlier, the pump tested had fixed throttling bushings as shaft seals. The seal injection was held in operation during the loss of suction transient. A mechanical seal might run dry during such a condition, unless specially designed to avoid this type of damage.

Obviously, it is impossible to simulate all different kinds of loss of suction transients which can occur in a plant, since every different plant layout of the feedwater system has its own advantages and weaknesses [15].

CONCLUSIONS

Rotordynamics

Summarizing, the following statements can be made:

- If properly designed, the throttling clearances (impeller labyrinths, balance piston, fixed throttling bushing shaft seals) in new condition provide a high amount of damping to the rotor.
- When clearances increase, shaft vibration amplitudes increase, hence stiffness and damping properties of the internal clearances deteriorate.

Nevertheless, the pump investigated showed no sign of a self excited subsynchronous vibration at twice design clearance.

- Unbalance excited vibration on the test pump was still low at twice design clearance.
- A swirl brake at the balance piston entrance drastically reduced the amplitude of unbalance excited vibrations. Installing throttling clearances with good stiffness and damping properties, together with introducing swirl brakes at selected locations, is one of the key design steps to obtain a good rotordynamic behavior.
- The fixed throttling bushes have a considerable damping effect on the rotor.
- Hydraulic excitation at rotational frequency ("hydraulic unbalance") exceeded by far the residual mechanical unbalance (G $\leq$ 2.5) for the pump "as built," even though precision cast impellers were used.
- At part load, there is a considerable rotor response due to subsynchronous broadband hydraulic excitation forces. In addition, the changing flow pattern due to recirculation strongly influences the synchronous vibration.
- With state-of-the-art analytical models, unbalance response can be predicted with reasonable accuracy. Forces considered have to include bearings, all throttling clearance effects, and impeller interaction.

Dry Running

- It could be demonstrated in the test, that the three-stage pump with its very rugged rotor design can sustain a "loss of suction" transient, starting with cavitation at the suction impeller and ending with a complete "steaming out" of the impeller/balance piston region, without difficulties.

In spite of surge like discharge pressure fluctuations of up to 150 bar, peak-to-peak rotor vibration amplitudes at the impeller of the first stage did not exceed ten percent of the labyrinth clearance.

REFERENCES

1. Florjancic, D., "Development and Design Requirements for Modern Boiler Feed Pumps," EPRI-CS-3158, Contract WE 81-211, Proceedings, pp. 4-74 (July 1983).
2. Massey, I. C., "Subsynchronous Vibration Problems in High-Speed, Multistage Centrifugal Pumps," *Proceedings of the Fourteenth Turbomachinery Symposium*, Turbomachinery Laboratory, Department of Mechanical Engineering, Texas A&M University, College Station, Texas (1985).
3. Valantas, R. A., and Bolleter, U., "Solutions to Abrasive Wear Related Rotordynamic Instability Problems on Prudhoe Bay Injection Pumps," *Proceedings of Fifth International Pump Users Symposium*, Turbomachinery Laboratory, Department of Mechanical Engineering, Texas A&M University, College Station, Texas (May 1988).
4. Bolleter, U., et al., "Predicting and Improving the Dynamic Behavior of Multistage High Performance Pumps," *Proceedings of First International Pump Symposium*, Turbomachinery Laboratories, Department of Mechanical Engineering, Texas A&M University, College Station, Texas (May 1984).
5. Childs, D. W., "Finite Length Solutions for Rotordynamic Coefficients of Turbulent Annular Seals," ASME-Paper 82-Lub-42 (1982).
6. Nordmann, R., et al., "Rotordynamic Coefficients and Leakage Flow for Smooth and Grooved Seals in Turbopumps," Proceedings IFToMM Meeting, Tokyo, Japan (1986).
7. Jery, B., et al., "Forces on Centrifugal Pump Impellers," *Proceedings of the Second International Pump Symposium*, Turbomachinery Laboratory, Department of Mechanical Engineering, Texas A&M University, College Station, Texas (1985).
8. Ohashi, H., et al., "Influence of Impeller and Diffuser Geometries on the Lateral Fluid Forces of Whirling Centrifugal Impellers," Workshop on Rotordynamic Instability Problems in High Performance Turbomachinery, Texas A&M University, College Station, Texas (1988).
9. Tsujimoto, Y., et al., "A Theoretical Study of Fluid Forces on a Centrifugal Impeller Rotating and Whirling in a Vaned Diffuser," Workshop on Rotordynamic Instability Problems in High Performance Turbomachinery, Texas A&M University, College Station, Texas (1988).
10. Bolleter, U., et al., "Hydraulic Interaction and Excitation Forces of High Head Pump Impellers," Proceedings of Third Joint ASCE/ASME Pumping Machinery Symposium, San Diego, California (1989).
11. MADYN Rotordynamic Computer Code, Ing. Büro Klement, Darmstadt, West Germany.
12. FEATURE Rotordynamic Computer Code, Mechanical Technology, Incorporated, Latham, New York.
13. Nikolajsen, J. L., and Gajan, R. J., "A New Computer Program for Pump Rotordynamic Analysis," *Proceedings of the Fifth International Pump Users Symposium*, Turbomachinery Laboratory, Department of Mechanical Engineering, Texas A&M University, College Station, Texas (1988).
14. Pace, S. E., et al., "Rotordynamic Developments for High Speed Multistage Pumps", *Proceedings of the Third International Pump Symposium*, Turbomachinery Laboratory, Department of Mechanical Engineering, Texas A&M University, College Station, Texas (1986).
15. de Vries, M., and Simon A., "Suction Effects on Feedpump Performance: A Literature Survey," EPRI Report CS-4204, Electric Power Research Institute, Palo Alto, California.
16. Guelich, J. F., et al., "Influence of Flow between Impeller and Casing on Part-Load Performance of Centrifugal Pumps," Proc. ASCE/ASME Pumping Machinery Symposium, San Diego, California (1989).
17. Guelich, J. F., European Patent EP 0 224 764 B1.
18. Nordmann, R., et al., "Finite Difference Analysis of Rotordynamic Seal Coefficients for an Eccentric Shaft Position," Proceedings of IMechE Conference on Vibrations in Rotating Machinery, Edinburgh, Scotland (1988).

ACKNOWLEDGEMENT

The work described herein was conducted partially under contract RP 1884-10 from the Electric Power Research Institute (EPRI), Palo Alto, California, under the project management of Stanley E. Pace and Tom McCloskey. The permission to publish the results of this investigation is gratefully acknowledged. The authors are thankful to all the members of the team at Sulzer Brothers, Limited., who have contributed to this work.